Kinetic Study of the Thermal Decomposition of Isocyanic Acid in Shock Waves

Okitsugu KAJIMOTO,† Osamu KONDO, Kazuo OKADA, Jiro FUJIKANE, and Takayuki FUENO*
Department of Chemistry, Faculty of Engineering Science, Osaka University, Toyonaka, Osaka 560
(Received May 25, 1985)

Thermal decomposition of isocyanic acid HNCO diluted to less than 2.0 mol% in argon was studied behind incident shock waves over the temperature range 2100—2500 K. The decomposition course was followed by monitoring the light absorption of HNCO and $NH(^3\Sigma^-)$ at 206 and 336 nm, respectively. It is confirmed that the primary step of the decomposition is a bimolecular process $HNCO+Ar \rightarrow NH(^3\Sigma^-)+CO+Ar$, $\Delta H^\circ_0=337$ kJ mol^{-1}, with the low-pressure limit rate constants $k=10^{17.23\pm0.36}\exp[-(402\pm17)\text{ kJ mol}^{-1}/RT]$ cm^3 mol^{-1} s^{-1}. The siglet-to-triplet crossing point is estimated on the basis of the RRKM low-pressure-limit rate constant calculations. The overall decomposition mechanism is suggested and its validity is confirmed by computer simulation of the time-concentration profiles of $NH(^3\Sigma^-)$ at varying temperature.

Decomposition of isocyanic acid (HNCO) as a possible source of the imino radical (NH) has already been investigated by several groups of workers. Holland *et al.*[1] first photolyzed HNCO to observe a strong absorption by NH. Wooley and Back[2] found that the primary process of the HNCO photolysis at 206.2 nm involves the following two branches with nearly equal probabilities:

$$\text{HNCO} + h\nu \longrightarrow \begin{cases} \text{NH} + \text{CO} \\ \text{H} + \text{NCO} \end{cases}$$

Pyrolysis of HNCO was also studied by Back and Childs[3] at the temperature range 550—770 °C. Unfortunately, however, the overall decomposition process was so complex because of the secondary reactions as well as the surface effects that the kinetic features of even the primary step remained to be disclosed.

In the present investigation, isocyanic acid diluted in argon has been decomposed in incident shock waves over the temperature range 2100—2500 K. Time-resolved measurements of the light absorptions of both reactant and product radicals at elevated temperatures greatly facilitated kinetic studies of the decomposition. Of the following three conceivable initial steps of decomposition:

		ΔH°_0(kJ mol^{-1})[5,6]	
HNCO + Ar	$\rightarrow NH(^1\Delta)+CO+Ar$	488	(1a)
	$\rightarrow NH(^3\Sigma^-)+CO+Ar$	337	(1b)
	$\rightarrow H+NCO+Ar$	474	(1c)

the spin-forbidden reaction 1b has been concluded to be the most dominant, just as in the case of the hydrazoic acid (HN_3) decomposition studied previously.[4] The overall decomposition mechanism was inferred on this basis, and its validity was confirmed from the computer tracing of the time histories of the $NH(^3\Sigma^-)$ concentrations at varying temperature.

Experimental

(A) Materials. Isocyanic acid was synthesized by heating a mixture of potassium cyanate and stearic acid for 8 h on an oil bath at 95 °C. All the volatile substances were collected in a trap maintained at −196 °C. Impurities that remained were carbon dioxide and water, which were removed by successive trap-to-trap distillations at −60 °C and −20 °C. Purity of the resulting isocyanic acid was checked by the mass,[9] IR,[10] and UV[11] spectrometries.

Sample gases of various concentrations (0.1—2.0 mol%) were prepared by diluting isocyanic acid with high purity (99.999%) argon. They were allowed to stand in 10-l Pyrex bulbs for at least 10 h before use. No trace of polymerization of HNCO was perceived in these diluted gas samples.

(B) Kinetic Measurements. A stainless-steel shock tube of 10.4 cm diameter was used. The driver and driven sections were 2.0 and 3.0 m in length, respectively. A 25-l dump tank was attached to the end wall of the driven section in order to prevent the driven gas from being heated further by reflected shock waves. An involatile substance was found to be formed near the end of the driven section unless such a tank was used. The two sections were separated by a Mylar diaphragm of 0.10, 0.18, or 0.25 mm thickness. The bursting pressures of these Mylar sheets were *ca.* 4, 7, and 10 atm,[12] respectively. The driven section was evacuated to less than 2×10^{-5} Torr[12] before charging it with a gas sample. A diaphragm of selected thickness was used in combination with a driver gas, H_2 or He, of given driven pressures, so that the net pressure of the reaction zone could vary from 500 to 1500 Torr. The temperature, pressure, and density of shocked gas were calculated from the measured shock velocity by assuming an ideal shock behavior. Both the boundary layer effects and the effects of reaction heat were estimated to be unimportant under our experimental conditions.

The light absorption at 206.2±2.8 nm was utilized to follow the concentration of HNCO. A home-made microwave-operated I_2 lamp, together with a Bausch-Lomb MC-20 grating monochromator, was used to isolate the 206.2 nm atomic line. The $NH(A^3\Pi\text{-}X^3\Sigma^-)$ absorption was also followed at the wavelength 335.96±0.14 nm.[13] A 400-W Ushio high-pressure mercury lamp and a Rikotsusho MC-50 grating monochromator were used for this purpose. The wavelength scale of the monochromator was calibrated by using an NH lamp[14] which was microwave-operated on a flowing mixture of 1 Torr of ammonia and 4 Torr of argon.

The light which passed an appropriate optical path was collected on an EMI-9634Q photomultiplier. Its time-dependent output signal was amplified with a Keithley 102B amplifier and stored in a Kawasaki Electronica TM-1450

†Present address: Faculty of General Education, The University of Tokyo, Meguro-ku, Tokyo 153.

transient memory. The stored signal was displayed on an oscilloscope for photographing or on a pen recorder.

Results

(A) Kinetics of the HNCO Decay. In all experiments, the HNCO absorption increased abruptly upon the arrival of incident shock wave, and then decreased gradually with elapsing time. At the shock wave temperatures above 2500 K, the effects of unidentified emission were found to be inevitable. Below 2200 K, on the other hand, the absorption often showed an irregular increase, especially when the pressure of the reaction zone exceeded 1000 Torr. Observations of the HNCO decay were thus limited to the temperature range between 2200 and 2500 K.

At temperatures between 2200 and 2500 K, the observed HNCO decay signals were smooth enough and well reproducible. It is believed that the initial decays of HNCO observed in this temperature region are entirely due to its decomposition effected by the shock heating. This point was corroborated from the observations of the concurrent increase in concentration of the NH radicals as the primary decomposition product, as will be demonstrated shortly below.

The absorption coefficient of HNCO at each experimental temperature was evaluated from the absorbance extrapolated to time zero and the calculated initial post-shock concentration of HNCO. The absorption coefficients thus obtained were essentially constant at $(1.37\pm0.20)\times10^5$ $cm^2 mol^{-1}$ over the temperature range studied.

By use of the average absorption coefficient $\varepsilon = 1.37\times10^5$ $cm^2 mol^{-1}$, the absorbance-time records were converted into concentration-time curves. First-order plots of the HNCO concentration against the particle time t were satisfactorily linear during the initial 100 μs. The first-order rate constants k_{1st} obtained from such plots for several typical runs are listed in Table 1, together with the relevant shock parameters.

Plots of log k_{1st} against $1/T$ gave three separate straight lines which were parallel-shifted upward as the total pressure P_2 was increased stepwise (500, 900, and 1300 Torr). The second-order rate constants k_{2nd} were obtained by dividing k_{1st} by the post-shock argon concentration. The values of k_{2nd} obtained for typical runs are given in the final column of Table 1.

The Arrhenius plots of k_{2nd} were found to give a single straight line. Figure 1 shows such plots for a total of 22 runs. Evidently, the HNCO decay is in the low-pressure region under our experimental conditions. The least-squares treatment of all the data given in Fig. 1 resulted in the following Arrhenius expression:

$$k_{2nd} = 10^{17.23\pm0.36} \exp[-(402\pm17)\text{kJ mol}^{-1}/RT] \quad \text{cm}^3\,\text{mol}^{-1}\,\text{s}^{-1}. \quad (1)$$

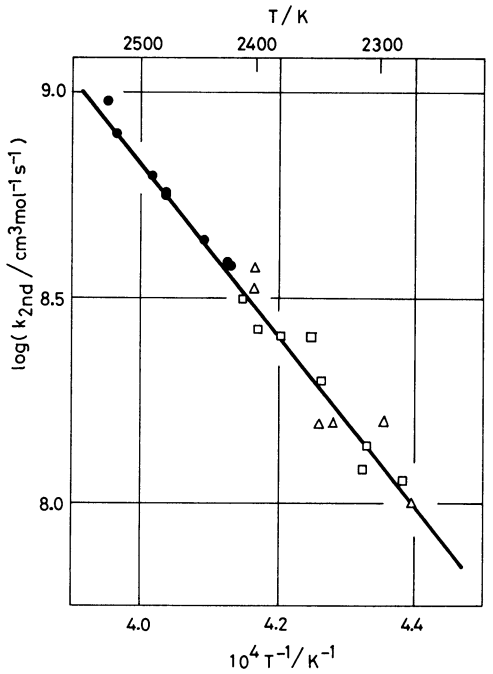

Fig. 1. Arrhenius plots of the second-order rate constants (k_{2nd}) for the decay of HNCO. The approximate Total pressures and the concentrations of HNCO in Ar were as follows: ●, 500 Torr, 2.0 mol%; □, 900 Torr, 0.5 mol%; △, 1350 Torr, 0.5 mol%.

TABLE 1. RATE DATA FOR THE SHOCK WAVE DECOMPOSITION OF HNCO

m	P_2	ρ_{21}	T_2	[Ar]	$[HNCO]_0$	k_{1st}	k_{2nd}
mol%	Toor		K	10^{-6} mol/cm^3	10^{-8} mol/cm^3	10^3 s^{-1}	10^8 cm^3 mol^{-1}s^{-1}
2.00	494	3.57	2523	3.07	6.27	2.41	7.86
2.00	511	3.56	2489	3.23	6.59	2.00	6.20
2.00	520	3.56	2478	3.30	6.73	1.95	5.61
2.00	528	3.55	2421	3.43	7.00	1.30	3.77
0.500	880	3.54	2411	5.82	2.93	1.83	3.14
0.500	892	3.53	2346	6.07	3.05	1.20	1.98
0.500	933	3.52	2282	6.52	3.28	0.735	1.13
0.500	1316	3.54	2401	8.75	4.50	3.20	3.66
0.500	1378	3.53	2337	9.41	4.73	1.48	1.57
0.500	1346	3.51	2275	9.44	4.74	0.965	1.02

TABLE 2. DATA FOR THE OBSERVATION OF THE $NH(^3\Sigma^-)$ ABSORPTION

m	P_2	ρ_{21}	T_2	[Ar]	$[HNCO]_0$	k_{1b}
mol%	Toor		K	10^{-6} mol/cm^3	10^{-8} mol/cm^3	10^8 cm^3 mol^{-1} s^{-1}
0.491	573	3.505	2230	4.12	2.02	0.532
0.498	555	3.471	2081	4.28	2.13	0.105
0.201	528	3.554	2526	3.35	0.674	8.78
0.201	516	3.536	2425	3.41	0.684	3.56
0.200	532	3.526	2281	3.94	0.788	0.902
0.200	996	3.495	2209	7.23	1.45	0.465
0.200	1052	3.469	2108	8.01	1.60	0.169
0.100	1375	3.546	2479	8.90	0.890	4.11
0.100	1469	3.503	2240	10.5	1.05	0.689
0.100	1523	3.490	2206	11.1	1.11	0.369

(B) Rate Constants for the $NH(^3\Sigma^-)$ Formation. Observation of the $NH(^3\Sigma^-)$ absorption at 336 nm was feasible at reaction temperatures down to 2100 K. At any temperature between 2100 and 2500 K, the absorption started up sharply upon the arrival of the incident shock. It increased monotonously until it reached a maximum, beyond which it decreased gradually. As the reaction temperature was raised, the absorption increased more abruptly, thus reaching its maximum in a shorter time interval and then decreasing faster. The maximum absorption became larger correspondingly. These qualitative features of absorption suffice to indicate an initial production of $NH(^3\Sigma^-)$ by the shock heating, followed by its decay due to subsequent reactions with coexistent species.[15]

The rates of the $NH(^3\Sigma^-)$ formation were evaluated from the initial slope of the absorption-time profile, assuming the average absorption coefficient $\varepsilon=1.0\times10^7$ cm^2 mol^{-1} for $NH(^3\Sigma^-)$.[4] The resulting rates were divided by the concentration product of Ar and HNCO, to obtain the second-order rate constant k_{1b}. The values of k_{1b} thus obtained for some representative runs are given in Table 2, together with the shock parameters.

Figure 2 shows the Arrhenius plots of k_{1b} obtained for a total of 31 runs. Irrespective of the total pressure ranging from 500 to 1500 Torr, all the experimental points are seen to be fitted by a single straight line. The results indicate that the unimolecular decomposition of HNCO into $NH(^3\Sigma^-)$+CO is in the low-pressure limit. The least-squares treatment of the data gave the following Arrhenius expression:

$$k_{1b} = 10^{17.38\pm0.29}\exp[-(412\pm13)\text{kJ mol}^{-1}/RT]\ \text{cm}^3\,\text{mol}^{-1}\,\text{s}^{-1}. \quad (2)$$

Shown with a dotted line in Fig. 2 is the k_{2nd}, Eq. 1. The essential agreement between these two lines can be taken as a strong indication that HNCO decomposes mostly into $NH(^3\Sigma^-)$+CO.

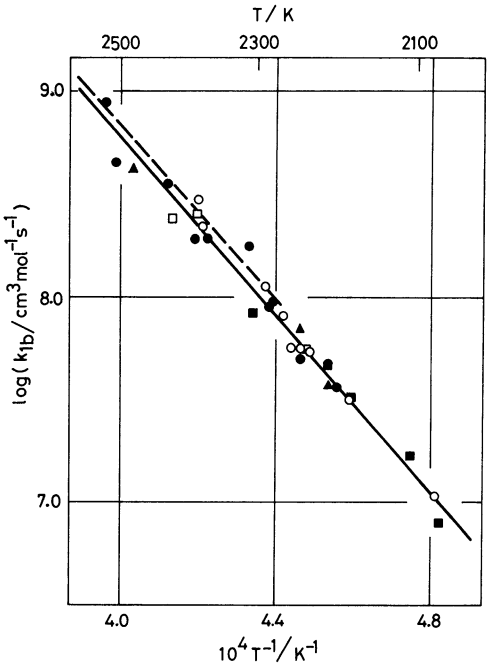

Fig. 2. Arrhenius plots of the second-order rate constants (k_{1b}) for HNCO+Ar→$NH(^3\Sigma^-)$+CO+Ar determined from the initial slope of the $NH(^3\Sigma^-)$ absorption. The approximate total pressures and the concentrations of HNCO in Ar were as follows: ○, 550 Torr, 0.5 mol%; ●, 550 Torr, 0.2 mol%; ■, 1000 Torr, 0.2 mol%; □, 1000 Torr, 0.1 mol%; △, 1500 Torr, 0.1 mol%. The rate constant of HNCO disappearance, k_{2nd}, is also shown with a dotted line.

Discussion

(A) Primary Decomposition Step. The close agreement between k_{2nd} and k_{1b} strongly suggests that HNCO is decomposed into $NH(^3\Sigma^-)$ and CO. The decomposition step is evidently bimolecular in type at least under our experimental conditions. The low-pressure limit behavior in the ordinary pressure regime has also been reported for other four-atomic molecules such as HN_3,[4] NH_3,[16] C_2N_2,[17,18] H_2O_2,[19] and SO_3,[20] diluted in inert gas.

The activation energy of k_{2nd}, E_a=402 kJ mol^{-1}, is noticeably greater than the heat of reaction $\Delta H°_0$=337 kJ mol^{-1} for the triplet path 1b but is clearly smaller than the heat of reaction $\Delta H°_0$=488 kJ mol^{-1} for the singlet path 1a. Similar situations have been noted in the thermal decompositions of HN_3[4] and N_2O,[21]

where the observed activation energies are in between the heats of reaction for the lowest triplet path and the higher singlet path.

In order to estimate the threshold energy for reaction 1b, we have undertaken RRKM calculations of the low-pressure limit rate constants:

$$k^{\mathrm{RRKM}} = (\lambda Z/Q_{\mathrm{v}})\exp(-E_0/RT)\int_0^{\infty} N(\varepsilon+E_0)\exp(-\varepsilon/RT)\mathrm{d}\varepsilon. \quad (3)$$

The various symbols appearing in Eq. 3 have their usual meanings.[22]

In calculating k^{RRKM}, we adopted the Whitten-Rabinovitch approximation[23] to $N(\varepsilon+E_0)$. The collision diameter between HNCO and Ar was assumed to be 0.39 nm. The six vibrational normal-mode frequencies of HNCO were all taken from the literature:[8] 3535, 2274, 1327, 808.0, 672.5, and 563.5 cm^{-1}.

We first calculated the k^{RRKM} as the functions of E_0 and T. Then we searched for a value of E_0 such that the observed temperature dependence of $k_{2\mathrm{nd}}$ (Eq. 1) was best reproduced. For the sake of simplicity, we neglected possible minor temperature dependence of the collisional efficiency λ. The best fit was achieved when we chose E_0=439 kJ mol^{-1}. The resulting RRKM rate constant was

$$k^{\mathrm{RRKM}} = \lambda 10^{17.76}\exp(-402\mathrm{kJ\ mol^{-1}}/RT)\ \mathrm{cm^3\ mol^{-1}s^{-1}}. \quad (4)$$

Comparison of Eq. 4 with Eq. 1 leads to the collisional efficiency λ=0.30. The λ value thus obtained does not seem to be unreasonable in view of the fact that the decompositions of most four-atomic molecules take on λ of the order of 0.1.[24] In addition, the critical energy E_0=439 kJ mol^{-1} of our choice suggests that the singlet and triplet potential energy curves cross each other at 102 kJ mol^{-1} *above* the zero point energy level of NH($^3\Sigma^-$)+CO. The situation is very similar to the case of HN_3.[4] The schematic potential energy diagrams for both cases are compared in Fig. 3.[25]

The critical energy E_0 for reaction 1b is smaller than the heats of reaction for paths 1a and 1c by 49 and 35 kJ mol^{-1}, respectively. Because reaction 1b of our major concern is found to be in the low-pressure limit region, the contributions of 1a and 1c to the decomposition are likely to be negligible under the experimental conditions adopted in this work.[26]

(B) Overall Decomposition Mechanism. On the basis of the previously reported results on the photolysis of HNCO[27,28] as well as the mechanism proposed for the pyrolysis of HN_3,[4] we here assume the overall mechanism of the HNCO thermal decomposition to be such as follows:

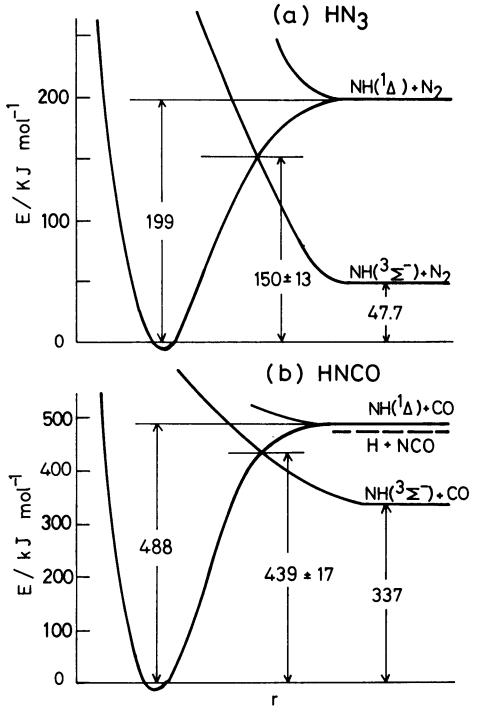

Fig. 3. Schematic potential energy curves of HN_3 (a) and HNCO(b).

		ΔH°_0(kJ mol^{-1})[5,6]
HNCO+Ar	$\xrightarrow{1b}$ NH($^3\Sigma^-$)+CO+Ar	337
NH($^3\Sigma^-$)+HNCO	$\xrightarrow{2}$ NH_2+NCO	99
H+HNCO	$\xrightarrow{3}$ NH_2+CO	−38
NH_2+HNCO	$\xrightarrow{4}$ NH_3+NCO	26
2NH($^3\Sigma^-$)	$\xrightarrow{5}$ N_2+2H	−272
2NH_2(+Ar)	$\xrightarrow{6}$ H_2NNH_2(+Ar)	−277
H+NH_2+Ar	$\xrightarrow{7}$ NH_3+Ar	−448
2H+Ar	$\xrightarrow{8}$ H_2+Ar	−432
NH($^3\Sigma^-$)+NH_2(+Ar)	$\xrightarrow{9}$ $HNNH_2$(+Ar)	−361
H+$HNNH_2$	$\xrightarrow{10}$ 2NH_2	−34
2NCO	$\xrightarrow{11}$ N_2+2CO	−546

In order to examine the validity of this mechanism, the simultaneous kinetic equations for the various species involved were solved numerically (GEAR method) on a computer. Specifically, we aimed at comparing the calculated time-concentration profiles of NH($^3\Sigma^-$) with the observed ones at varying temperature. The rate constants used for computations are summarized in Table 3. Most of these data were either taken directly from the literature[29-31] or estimated judiciously by the procedures analogous to those delineated previously for the case of HN_3.[4]

The time-concentration profiles of NH($^3\Sigma^-$) were

TABLE 3. RATE CONSTANTS USED FOR COMPUTER SIMULATION OF THE HNCO DECOMPOSITION

Reaction	Rate constant ($cm^3\,mol^{-1}\,s^{-1}$)	Reference
1b	$k_{1b}=10^{17.23}\exp(-402\,kJ\,mol^{-1}/RT)$	This work
2	$k_2=10^{11.5}\exp(-106\,kJ\,mol^{-1}/RT)$	a)
3	$k_3=10^{11}$	a)
4	$k_4=10^{11.5}\exp(-50\,kJ\,mol^{-1}/RT)$	a)
5	$k_5=2.0\times10^{13}$	b)
6	$k_6=1.5\times10^{13}$	29)
7	$k_7=2.2\times10^{15}$ [Ar]	30)
8	$k_8=6.5\times10^{17}\,T^{-1}$ [Ar]	31)
9	$k_9=1.5\times10^{13}$	a)
10	$k_{10}=10^{11}$	a)
11	$k_{11}=10^{12}$	a)

a) Estimated, b) Adjusted.

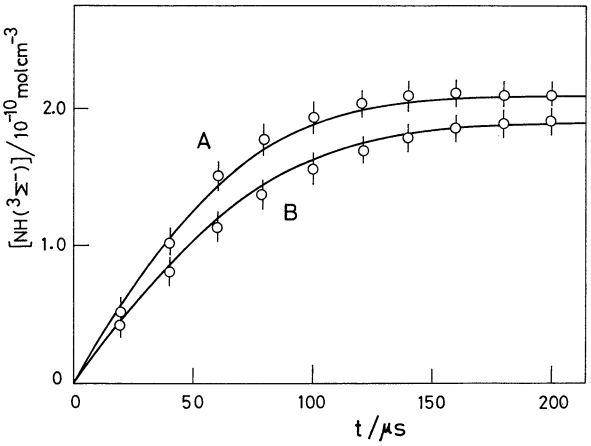

Fig. 4. Comparisons of the computed NH($^3\Sigma^-$) concentration profiles (——) with the observed (○): (A)NHCO=0.20 mol%, T_2=2281 K, P_2=532 Torr; (B) HNCO=0.20 mol%, T_2=2108 K, P_2=1052 Torr. The vertical lines indicate the range of uncertainty due to the low S/N ratio.

found to be governed by the rates of the initial process 1b and the NH "recombination" reaction 5. The rate constants for reactions 6—8, 10, and 11 had virtually no effects on the calculated profiles. In practice, we adopted k_{2nd} (Eq. 1) rather than k_{1b} (Eq. 2) as the rate constant for reaction 1b since there may well exist some uncertainty in the absorption coefficient of NH($^3\Sigma^-$). The rate constant of reaction 5 was most influential in the determination of the position as well as the height of the peak of the calculated profiles. We thus adjusted the value of k_5 so as to best reproduce the observed profiles of NH($^3\Sigma^-$) at various temperatures studied. The best fit was obtained when k_5 was taken to be constant at 2×10^{13} $cm^3\,mol^{-1}\,s^{-1}$ within the temperature range studied. This value agrees well with 2.5×10^{13} $cm^3\,mol^{-1}\,s^{-1}$ adopted previously.[4]

Figure 4 shows examples of the calculated time histories of the NH($^3\Sigma^-$) concentration. Circles shown in Fig. 4 are the concentrations calculated from the observed absorption profiles of NH($^3\Sigma^-$) by using $\varepsilon=1.0\times10^7$ $cm^2\,mol^{-1}$ as the absorption coefficient of NH($^3\Sigma^-$). Agreements between the calculated curves and the observed are satisfactory. The results lend strong support not only to the overall decomposition mechanism assumed but also to the various assumptions invoked as well as the experimental techniques adopted in the present work.

In conclusion, the primary process of the shock-wave decomposition of HNCO in argon at the total pressure range 550—1500 Torr is a bimolecular reaction, giving rise exclusively to NH($^3\Sigma^-$). The activation energy E_a=402 kJ mol^{-1} for this "triplet" process is evidently higher than its heat of reaction $\Delta H°_0$=337 kJ mol^{-1}, indicating that the singlet-triplet potential-energy curve crossing occurs at a level above the dissociation limit. The kinetic behavior is found to conform to the RRKM theory in the low-pressure limit.

This work was supported in part by the Grant-in-Aid for Scientific Research No. 59030074 from the Ministry of Education.

References

1) R. Holland, R. N. Dixon, D. A. Ramsay, and D. W. G. Style, *Nature*, **182**, 336 (1958).

2) W. D. Wooley and R. A. Back, *Can. J. Chem.*, **46**, 295 (1968).

3) R. A. Back and J. Childs, *Can. J. Chem.*, **46**, 1023 (1968).

4) O. Kajimoto, T. Yamamoto, and T. Fueno, *J. Phys. Chem.*, **83**, 429 (1979).

5) The heats of reaction, $\Delta H°_0$, given in this paper are all based primarily on the relevant heat-of-formation data taken from S. W. Benson, "Thermochemical Kinetics," 2nd ed., John Wiley, New York (1976).

6) Piper[7] reviewed the thermochemical data on the heat of formation for the NH radical critically, concluding that the value given in JANAF Table,[8] 377 kJ mol^{-1} for $\Delta H°_{f0}$, must be lowered to 352 kJ mol^{-1}. In the present paper, all the thermochemical values pertaining to the NH radical have been based on this new value.

7) L. G. Piper, *J. Chem. Phys.*, **70**, 3417 (1979).

8) D. R. Stull and H. Prophet, "JANAF Thermochemical Tables," 2nd ed, Nationsl Bureau of Standards, Washington, D. C. (1971).

9) J. Y. P. Mui and R. A. Back, *Can. J. Chem.*, **41**, 826 (1963).

10) G. Herzberg and C. Reid, *Disc. Faraday Soc.*, **9**, 92

(1950).

11) R. N. Dixon and G. H. Kirby, *Trans. Faraday Soc.*, **64**, 2002 (1968).

12) 1 atm=101325 Pa and 1 Torr=(1/760) atm.

13) J. M. Lentz, *J. Quant. Spectrosc. Radiant Transfer*, **13**, 297 (1973).

14) I. Hansen, K. Höninghaus, C. Zetzsch, and F. Stuhl, *Chem. Phys. Lett.*, **42**, 370 (1976).

15) These features alone can by no means rule out the possibility that HNCO is first decomposed to give rise to $NH(^1\Delta)$, which is then rapidly quenched to $NH(^3\Sigma^-)$ on collisions with the reactant HNCO. In our previous investigation of the HN_3 decomposition,[4] we considered such a process beside the process giving $NH(^3\Sigma^-)$ directly. However, the conclusion was that the triplet path was evidently preponderant over the singlet path under the experimental conditions adopted there. Whether or not the triplet path is the major step of the initial decomposition in the present HNCO case also, is to be judged cautiously from the magnitudes as well as the temperature dependences of the rate constants observed for both the HNCO decay and the $NH(^3\Sigma^-)$ production.

16) K. W. Michael and H. Gg. Wagner, Proceeding of the 10th Internat. Symp. Combust., **1964**, 353 (1965).

17) W. Tsang, S. H. Bauer, and M. Cowperthwait, *J. Chem. Phys.*, **36**, 1768 (1962).

18) T. Fueno, K. Tabayashi, and O. Kajimoto, *J. Phys. Chem.*, **77**, 575 (1973).

19) H. Kijewski and J. Troe, Int. *J. Chem. Kinet.*, **3**, 223 (1971).

20) D. C. Astholz, K. Glänzer, and J. Troe, *J. Chem. Phys.*, **70**, 2409 (1979).

21) J. Troe and H. Gg. Wagner, in "Physical Chemistry of Fast Reactions," ed by B. P. Levitt, Plenum Press, London (1973), Vol. 1, p. 1.

22) P. J. Robinson and K. A. Holbrook, "Unimolecular Reactions," Willey-Interscience, London (1972).

23) G. Z. Whitten and B. S. Rabinovitch, *J. Chem. Phys.*, **38**, 2466 (1963).

24) The formal spin "forbiddenness" of the present triplet reaction should not be taken literally as such. Even though the spin is certainly not conserved during the decomposition, the reaction is in reality a unimolecular process in its low-pressure limit, where the thermal activation step is rate-controlling. The activation step itself would not necessarily involve the spin conversion.

25) The thermochemical values used in our previous study of HN_3 decomposition[4] have been recalculated according to Piper's heat of formation for NH,[6] and the values thus modified are given in Fig. 3(a).

26) The RRKM rate constants calculated for reactions 1a and 1c are indeed an order of magnitude smaller than the observed rate constants (1) and (2).

27) R. A. Back, *J. Chem. Phys.*, **40**, 3493 (1964).

28) N. J. Friswell and R. A. Back, *Can. J. Chem.*, **46**, 527 (1968).

29) P. V. Khe, J. C. Soulignac, and R. Lesclaux, *J. Phys. Chem.*, **81**, 210 (1977).

30) S. Gordon, W. Mulac, and P. Nangia, *J. Phys. Chem.*, **75**, 2087 (1971).

31) D. L. Baulch, D. D. Drysdale, D. G. Horne, and A. C. Lloyd, "Evaluated Kinetic Data for High Temperature Reactions," Butterworths, London (1972) Vol. 1.